PNAS
www.pnas.org

Supplementary Information for

Structural insights into α-synuclein monomer-fibril interactions

Pratibha Kumari[a,1], Dhiman Ghosh[a,1], Agathe Vanas[a], Yanick Fleischmann[a], Thomas Wiegand[a], Gunnar Jeschke[a], Roland Riek[a,2], and Cédric Eichmann[a,b,2]

[a]Department of Chemistry and Applied Biosciences, Laboratory of Physical Chemistry, ETH Zurich, 8093 Zurich, Switzerland

[b]Department of Biological Regulation, Weizmann Institute of Science, 76100 Rehovot, Israel

[1]P.K. and D.G. contributed equally to this work.

[2]To whom correspondence may be addressed. E-mail: roland.riek@phys.chem.ethz.ch or cedric.eichmann@phys.chem.ethz.ch

This PDF file includes:

Figures S1 to S8

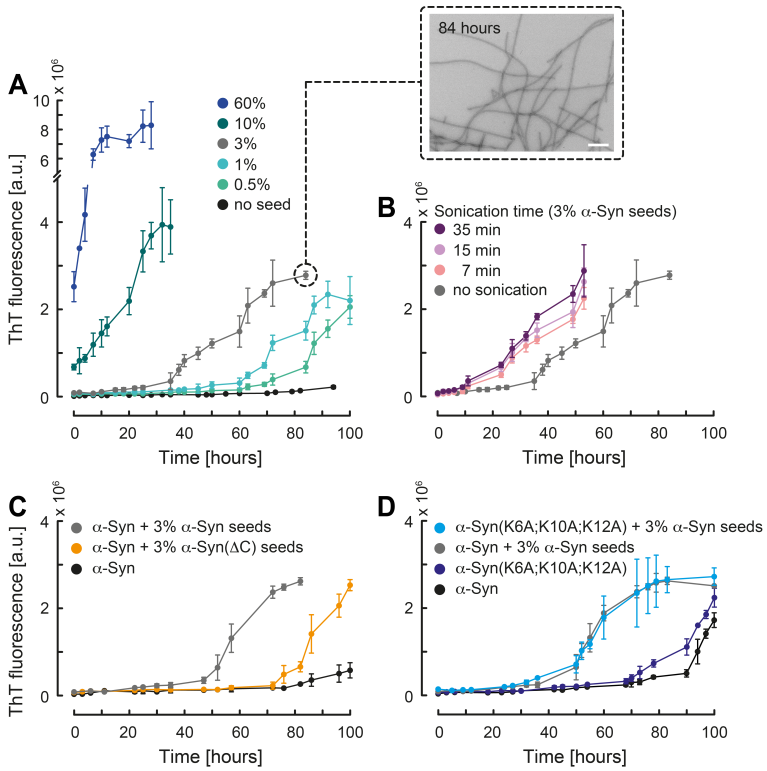

Fig. S1. Secondary nucleation of α-Syn at pH 7. (**A**) Seeded aggregation kinetics of wild-type α-Syn aggregation at constant monomer concentration with systematic variation of α-Syn seeds from 0-60% (expressed as percentage of the concentration of monomeric α-Syn) under quiescent conditions using mature fibrils without sonication at 37 °C. Inset, negative-stain EM of the ThT sample containing 3% seeds after 84 h of incubation, scale bar 400 nm. (**B**) Aggregation of wild-type α-Syn in absence and presence of 3% sonicated seeds, sonication time 7, 15, and 35 min. (**C**) Aggregation kinetics of wild-type α-Syn in absence and presence of 3% wild-type and α-Syn(ΔC) seeds. (**D**) Comparison of wild-type and mutant α-Syn(K6A;K10A;K12A) aggregation with and without addition of 3% wild-type α-Syn seeds. Monomer sample concentrations are 300 μM. Error bars denote standard deviations based on measurements on two independent replicate samples.

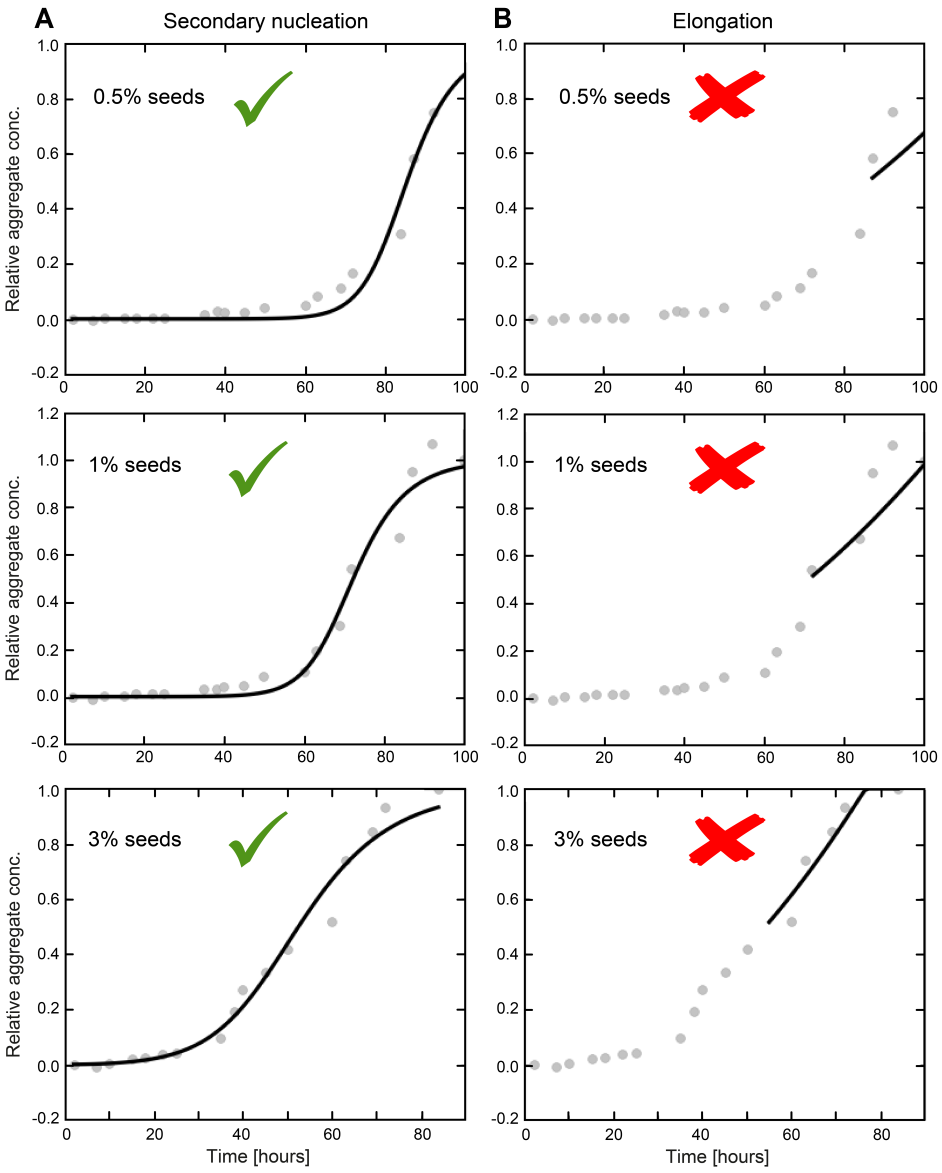

Fig. S2. Mechanisms of α-Syn aggregation. Global fitting of seeded wild-type α-Syn aggregation kinetics at pH 7 is consistent with (**A**) surface-catalyzed secondary nucleation but not with (**B**) elongation of fibrils.

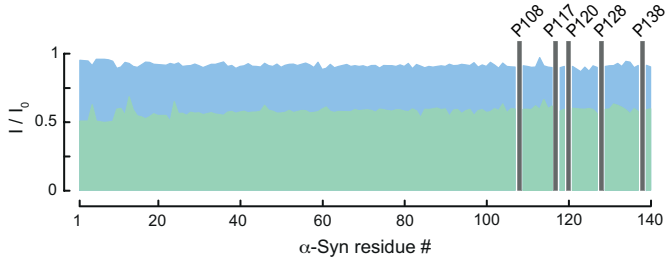

Fig. S3. Aggregation of monomeric α-Syn in presence of fibrils. Residue-resolved NMR signal intensity ratios (I/I_0) of monomeric α-Syn before (I_0) and after 5 h (I) incubation with 5.4-fold molar excess of α-Syn fibrils at pH 7 (blue) and pH 6 (green). Positions of C-terminal α-Syn proline residues without peptide amide resonances are shown in one-letter amino acid code.

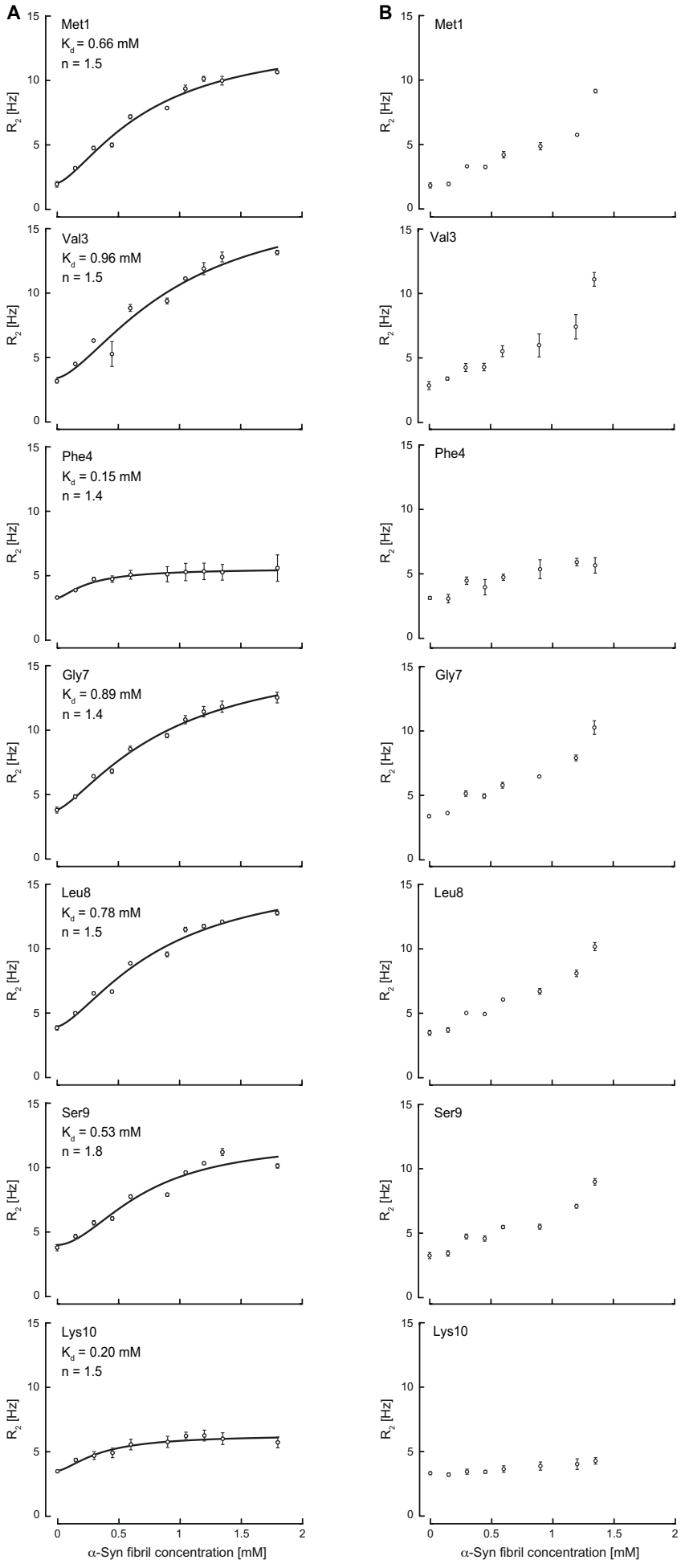
A
B
Met1
K_d = 0.66 mM
n = 1.5
Val3
K_d = 0.96 mM
n = 1.5
Phe4
K_d = 0.15 mM
n = 1.4
Gly7
K_d = 0.89 mM
n = 1.4
Leu8
K_d = 0.78 mM
n = 1.5
Ser9
K_d = 0.53 mM
n = 1.8
Lys10
K_d = 0.20 mM
n = 1.5
R_2 [Hz]
0
5
10
15
0
0.5
1
1.5
2
α-Syn fibril concentration [mM]

Fig. S4. Kinetics of α-Syn fibril interaction. ^{15}N R_2 relaxation rates of N-terminal α-Syn residues in presence of increasing concentration of α-Syn fibrils at (**A**) pH 7 were fitted by a hyperbolic binding function $r = a + b*n[\alpha\text{-Syn fibril}]^n/(K_d + [\alpha\text{-Syn fibril}]^n)$, n = number of fibril binding sites. (**B**) At pH 6, fast α-Syn aggregation upon addition of α-Syn fibrils did not allow fitting of the R_2 data to determine K_d values.

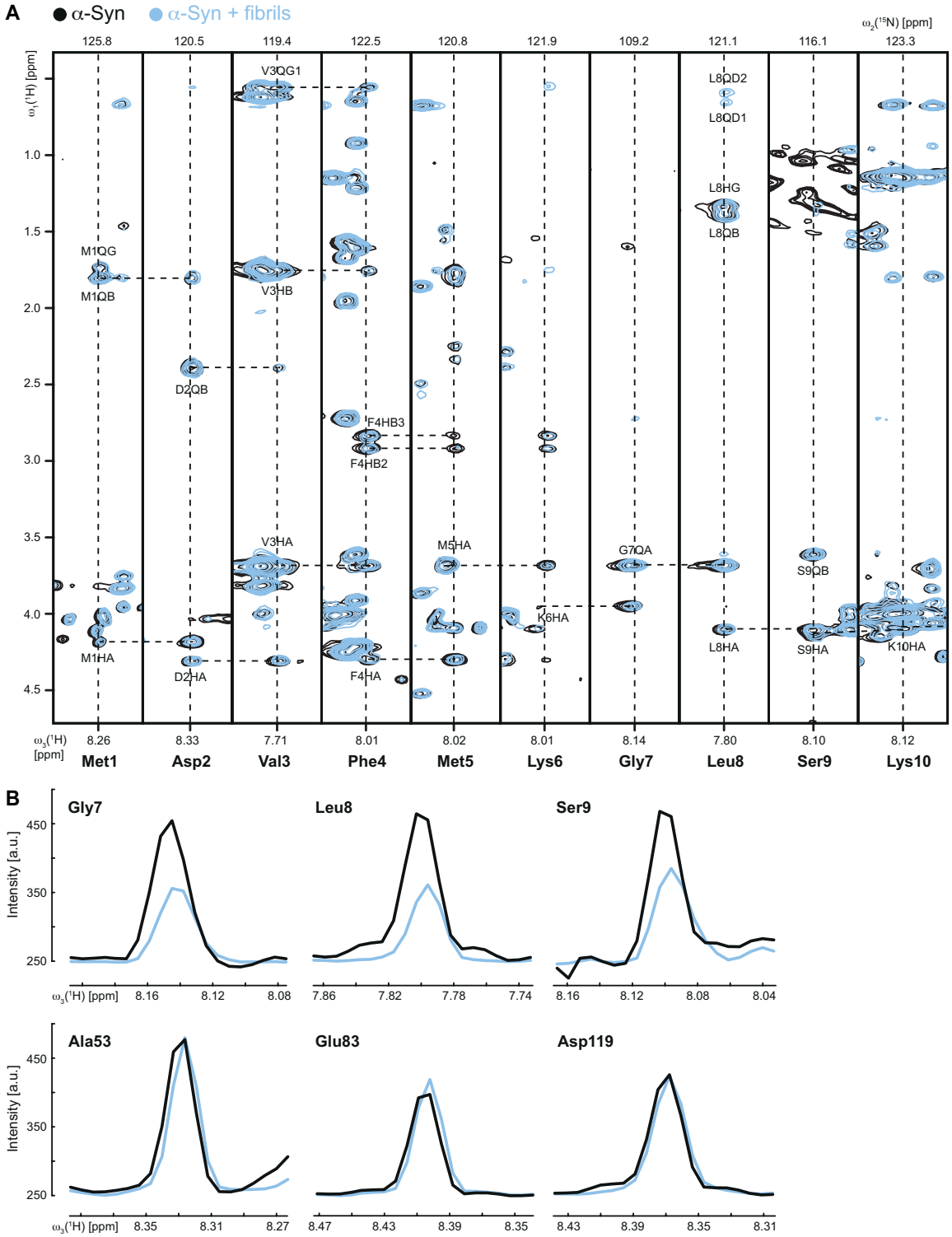

Fig. S5. Absence of structural features in transiently fibril-bound α-Syn. (**A**) $\omega_1(^1H)/\omega_3(^1H)$ strips obtained from 3D ^{15}N-resolved [^1H,^1H]-NOESY experiments for the 10 N-terminal residues of monomeric α-Syn in absence (black) and presence of α-Syn fibrils (blue, 6.7-fold molar excess of fibrils) at pH 7. The strips are centered about the amide proton chemical shifts and taken at the ^{15}N chemical shifts of the amide groups

for the indicated residues. (**B**) 1D $\omega_3(^1H)$ cross sections of the diagonal peak intensities from the NOESY spectrum.

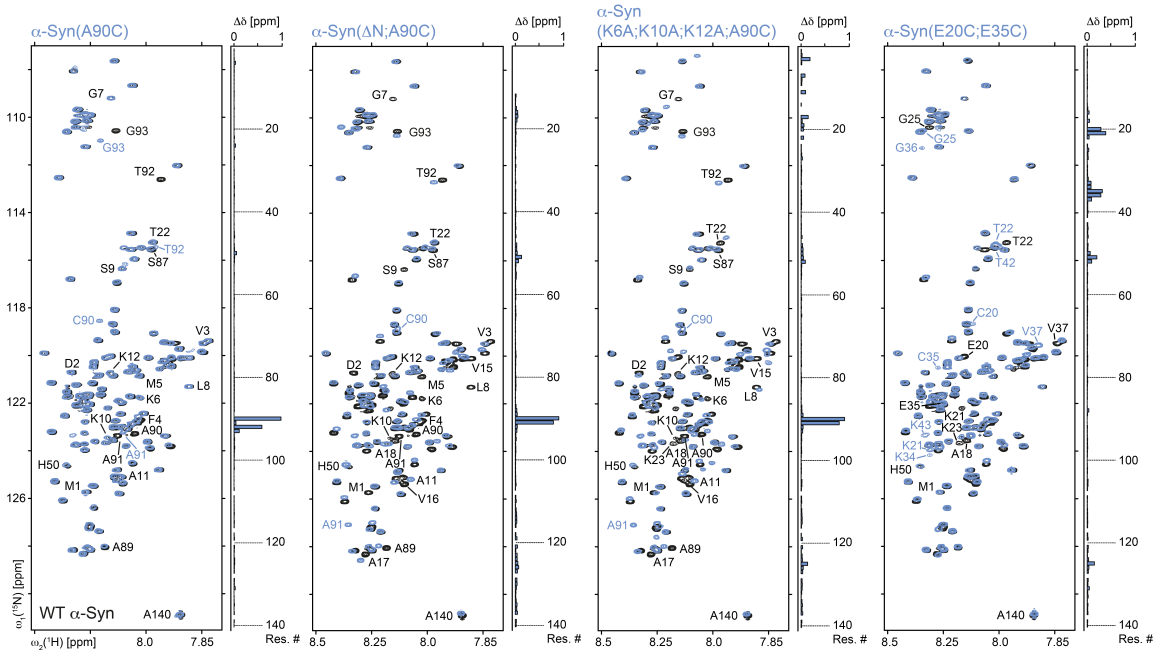

Fig. S6. Wild-type and α-Syn cysteine mutants are intrinsically disordered. Overlay of 2D NMR spectra of α-Syn(A90C), (ΔN;A90C), (K6A;K10A;K12A;A90C), and (E20C;E35C) (blue) with wild-type (WT) α-Syn (black) at pH 7. Chemical shift differences Δδ of non-proline backbone ^{15}N-^{1}H resonances between wild-type and α-Syn mutants were calculated as $\Delta\delta = [(\Delta\delta_{1H})^2 + (\Delta\delta_{15N} \times 0.2)^2]^{1/2}$. Residues without Δδ values were not analyzed because of missing cross-peak assignment.

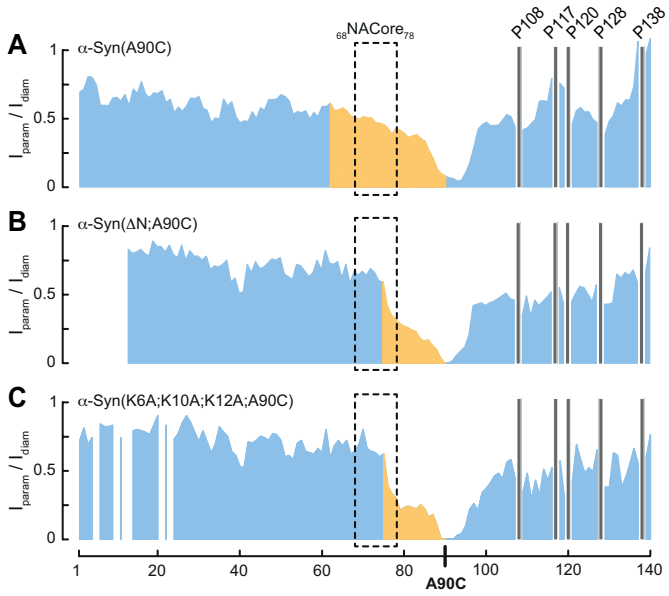

Fig. S7. PRE of α-Syn mutants. Residue-resolved PRE intensity profiles I_{param}/I_{diam} of para- (I_{param}) and diamagnetic (I_{diam}) labeled (**A**) α-Syn(A90C), (**B**) α-Syn(ΔN;A90C) and (**C**) α-Syn(K6A;K10A;K12A;A90C) at pH 7. Positions of C-terminal α-Syn proline residues without peptide amide resonances are shown in one-letter amino acid code.

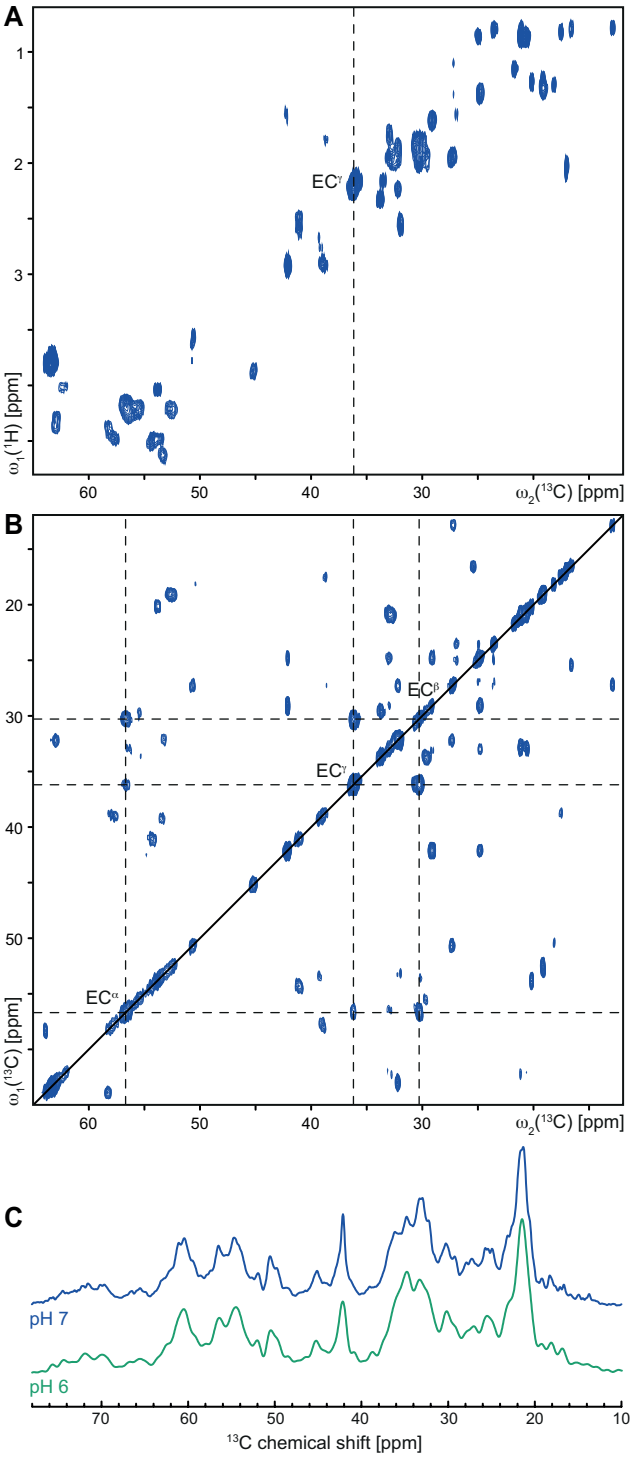

Fig. S8. Solid-state NMR assignment of the Glu side-chain atoms in the mobile region of α-Syn fibrils. (**A**) 2D ^{1}H-^{13}C INEPT spectrum of α-Syn fibrils. The cross-peak of Glu ^{13}C$^{\gamma}$ is indicated. (**B**) 2D ^{13}C-^{13}C INEPT-TOBSY spectrum of α-Syn fibrils showing the spin system of the Glu side-chain. (**C**) 1D ^{13}C MAS CP NMR spectra of α-Syn fibrils at pH 7 (blue) and 6 (green). Salt-free conditions.